Science Bulletin 68 (2023) 897–901

Contents lists available at ScienceDirect

Science Bulletin

journal homepage: www.elsevier.com/locate/scib

Short Communication

Decoupled orbital-scale variability of late Pleistocene-Holocene monsoonal circulation and rainfall in East Asia

Liya Jin [a,b,*], Andrey Ganopolski [c], Matteo Willeit [c], Huayu Lu [d], Fahu Chen [b,e], Xiaojian Zhang [d,*]

[a] School of Atmospheric Sciences, Chengdu University of Information Technology, Chengdu 610225, China
[b] Key Laboratory of Western China's Environmental Systems (Ministry of Education), College of Earth and Environmental Sciences, Lanzhou University, Lanzhou 730000, China
[c] Potsdam Institute for Climate Impact Research, Potsdam 14412, Germany
[d] School of Geography and Ocean Science, Frontiers Science Center for Critical Earth Material Cycling, Nanjing University, Nanjing 210023, China
[e] Alpine Paleoecology and Human Adaption Group, Key Laboratory of Alpine Ecology, Institute of Tibetan Plateau Research, Chinese Academy of Sciences, Beijing 100101, China

ARTICLE INFO

Article history:
Received 13 July 2022
Received in revised form 21 March 2023
Accepted 22 March 2023
Available online 6 April 2023

The East Asian summer monsoon (EASM) is a critical component of the global climate system due to its association with rainfall in areas hosting over one sixth of the global population [1]. Understanding the periodicities of summer rainfall influenced by the EASM can help constrain future climate projections. However, mechanisms of the response of the EASM associated summer rainfall variability to orbital forcing during the late Pleistocene-Holocene remains uncertain [2,3]. For example, EASM variability recorded by speleothem $CaCO_3$ oxygen-isotope ($\delta^{18}O$) records generally exhibits predominant 23- and 19-ka (1 ka = 1000 years) cycles over the past 640 ka. These covary with precession-driven, low-latitude summer insolation forcing [4]. However, Chinese loess magnetic susceptibility and ^{10}Be records covary with global ice volume variations and atmospheric CO_2 concentrations over the past 800 ka. Their predominant 100- and 41-ka cycles indicate the role of high-latitude forcing on glacial-interglacial timescales [5,6]. The 100-ka cycle resembles the eccentricity of the Earth's orbit but it makes a smaller contribution to insolation variation than that of the Earth's precession. Researchers refer to the discrepancy in orbital-scale EASM variability recorded by Chinese loess and cave speleothem $\delta^{18}O$ records as the "Chinese 100-ka problem" [2]. The timing of the Holocene EASM maximum also remains under dispute. Loess and pollen records document a mid-Holocene maximum while speleothem $\delta^{18}O$ records record an early-Holocene maximum [4,7,8]. Previous modeling studies on the evolution of EASM rainfall have estimated the relative contributions of external forcings (e.g., insolation, CO_2, ice sheets, etc.) in EASM rainfall variation. However, the periodicities and ultimately driving factors illustrated taken from long-term transient simulations are still rare.

This study generated an 800-ka long series of precipitation estimates over East Asia extracted from 3-Ma (1 Ma = 1,000,000 years) multiple transient simulations by the CLIMBER-2 intermediate complexity Earth system model (Figs. S1 and S2 online) [9]. The CLIMBER-2 model simulates correct present-day summer precipitation pattern (Fig. S3 online), and magnitude and timing of the last eight glacial cycles with respect to both global ice sheet volume (expressed in $\delta^{18}O$) and CO_2 concentrations (Fig. S4 online). Both the simulation and reconstructions [10,11] exhibit predominant 100- and 41-ka cycles in global ice sheet volume and CO_2 concentrations, although precession (23- and 19-ka) bands dominate high-latitude summer insolation (Fig. S4a online). In addition, both global ice volume (Fig. S4b online) and CO_2 concentrations (Fig. S4d online) from reconstructions show a transition (the so-called mid-Brunhes event) from low amplitudes (cool interglacial) to high amplitudes (warm interglacial) at ~430 ka [10,11]. This climatic transition is also captured by the ice sheet volume (Fig. S4c online) and CO_2 concentrations (Fig. S4e online) from the simulations. The CLIMBER-2 however generates this climatic transition at ~340 ka, significantly later than the reconstructed proxy estimate at ~430 ka (Fig. S4b, d online). The temporal gap may arise from biases in the transient simulation.

The EASM intensity is traditionally measured as monsoonal circulation expressed by low-level, southerly winds over East Asia in summer [1]. In the CLIMBER-2 simulation output, the EASM circulation index is calculated as average southerly winds at 850 hPa in summer from three CLIMBER grid cells centered at (15°N, 120°E), (25°N, 120°E), and (35°N, 120°E) (Fig. S3 online). These exhibit pronounced 19- and 23-ka cycles implying strong low-latitude modulation by precession. The circulation index also exhibits a weak 41-

* Corresponding authors.
E-mail addresses: jinly@lzu.edu.cn (L. Jin), zhangxj@nju.edu.cn (X. Zhang).

https://doi.org/10.1016/j.scib.2023.04.004
2095-9273/

ka cycle and no significant 100-ka cycle (<95% confidence level) (Fig. 1a) to resemble the $\delta^{18}O$ record of Sanbao Cave (Fig. 1b). Cross-spectral analysis further confirms strong coherence between model and proxy at 19- and 41-ka bands (Fig. S5a online). However, the simulated phase of the EASM circulation index lags behind that of the proxy record. This EASM circulation index also matches well with that simulated by the CCSM3 with the forcing of orbital parameters, greenhouse gas concentrations, and ice sheets over the past 300 ka (Fig. S6a, b online). The peak of the EASM circulation index appears during the early Holocene (Fig. S7a online) and resembles results of the TraCE-21ka simulation by the CCSM3 (Fig. S7b online) as well as the $\delta^{18}O$ record of Sanbao Cave (Fig. S7c online).

Simulated boreal summer rainfall in East Asia, denoted as "EASM rainfall", represents the average rainfall of two CLIMBER grid cells centered at (25°N, 120°E) and (35°N, 120°E) (Fig. S3 online). In contrast to the EASM circulation result, EASM rainfall shows pronounced 41- and 100-ka cycles (Fig. 1c) resembling the magnetic susceptibility record from the Xifeng Loess in northern China over the past 800 ka (Fig. 1d). The dominant 100-ka cycle also appears in snail $\delta^{13}C_{shell}$ records from the Xifeng Loess of northern China, the pollen record of Taihu Lake in central China, and the clay mineralogical record of Core MD12-3432 from the northern South China Sea (Fig. S8 online). Cross-spectral analysis also shows good model and proxy agreement although some differences in phase do appear (Fig. S5b online). However, the pronounced 100-ka cycle appearing in EASM rainfall (Fig. S6c online) did not appear in the CCSM3-300ka and CLIMBER2-650-ka transient simulations for the past 300 ka (Fig. S6d online), despite the fact that these simulations are forced by greenhouse gas concentrations and ice sheets subjected to the influence of the 100-ka cycle. The simulation results described here also exhibit an EASM rainfall peak during the mid-Holocene (Fig. S7d online). This contrasts with results from the TraCE-21ka and CLIMBER2-650ka simulations (Fig. S7e online) but resembles a pollen record from Gonghai Lake in northern China [7] (Fig. S7f online). Similarly timed mid-Holocene EASM maxima appear in proxy records from central, southeastern, and southern China (Fig. S9 online).

Precession bands appear much weaker in EASM rainfall compared to 100- and 41-ka bands over the past 800 ka. The main periodicities appearing in EASM rainfall resemble those from the Xifeng section (35.7°N, 107.6°E) loess record [5] (Fig. 1d) but differ from those recorded by the Sanbao Cave (31.67°N, 110.43°E) $\delta^{18}O$ record [4]. The latter record shows pronounced precession cycles without significant 100- and 41-ka cycles at the 95% confident level (Fig. 1b). The simulated EASM rainfall shows a transition from low amplitudes to high amplitudes at ~340 ka (Fig. 1c). The climatic transition recorded by the Xifeng Loess record occurred at ~550 ka (Fig. 1d), much earlier than the simulated result.

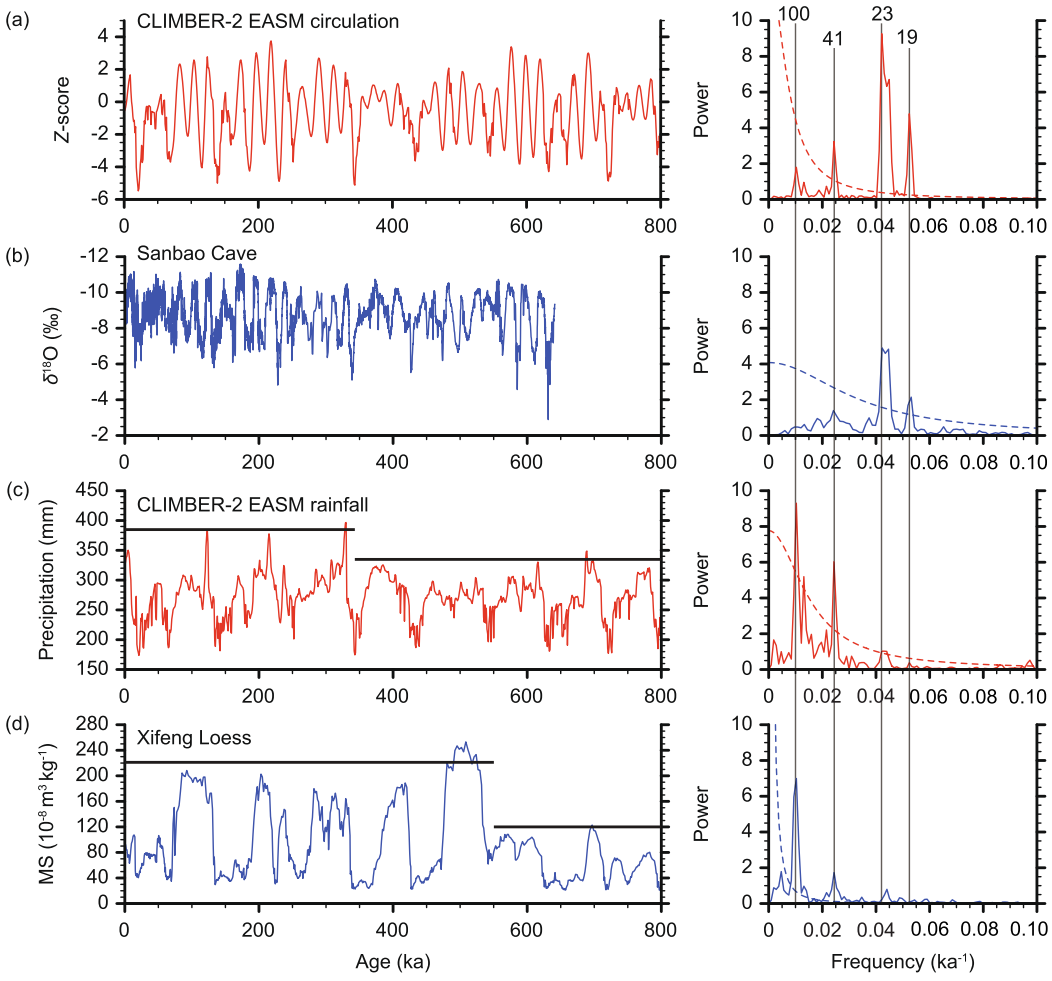

Fig. 1. (Color online) Proxy-model comparison of EASM variability during the past 800 ka: time series (left panel) and spectra (right panel). (a) Simulated EASM circulation index. (b) Sanbao Cave $\delta^{18}O$ (‰) [4]. (c) Simulated EASM rainfall (mm). (d) Magnetic susceptibility (MS, 10^{-8} m^3 kg^{-1}) record of the Xifeng Loess [5]. Black lines show the climatic transition in terms of the amplitude (left panel). Dashed lines indicate the 95% confidence level (right panel).

The simulation results indicate decoupling of EASM rainfall and circulation. This could explain differences in proxy records. This also does not support a delayed ecosystem response to EASM rainfall during the Holocene [8]. The decoupling between EASM rainfall and circulation could also reflect complex behavior of the EASM system on glacial–interglacial timescales. Modern climate data indicate that the EASM onset in mid-May initiates the pre-flood season of southern China which continues into early June. The ensuing Meiyu season in China, Korea, and Japan runs from mid-June to early July and transitions into the rainy season of northern China from mid-July to late August. The rain belt reaches the northernmost areas of China during boreal summer. The rainfall in East Asia is generally formed by frontal systems. These develop when warm, moist air flows brought by the monsoonal southwesterlies and southeasterlies meet cold air masses brought by the westerlies. Climatologically, the seasonal transition of the summer rainfall belt is accompanied by the northward shift of the western North Pacific subtropical high (WNPSH) system. Areas near the ridgeline of the WNPSH experience hot, sunny days due to descending, dry air (divergence), while a frontal belt develops in areas along western and northwestern flanks of the WNPSH (Fig. S10 online). EASM rainfall thus results from the interplay between monsoonal and westerly circulations.

For the past 800 ka, monsoonal moisture transport calculated as the average of summer southerly moisture flux at 850 hPa of three model grid cells (15°N, 120°E; 25°N, 120°E; 35°N, 120°E) shows significant 23- and 19-ka cycles (Fig. 2a). Moisture transport is controlled by the monsoonal southerlies, i.e., EASM circulation (Fig. 1a). Stronger southerlies transport more moisture from the tropical Pacific and Indian Oceans to East Asia. This moisture transport distance is greater than that from the Northwest Pacific, an area that also contributes rainfall in East Asia (Fig. S10 online). Moisture becomes depleted in ^{18}O with increasing transport distance due to enhanced rainout via Rayleigh distillation processes. Stronger southerly transport leads to more ^{18}O-depleted moisture in East Asia and lower $\delta^{18}O$ values in stalagmites. Stalagmite $\delta^{18}O$ variability thus likely reflects EASM circulation. Differences in EASM rainfall and circulation variation indicate that EASM circulation related moisture transport is not the dominant mechanism controlling glacial–interglacial changes in EASM rainfall. In addition to EASM circulation, some research cites the impact of mid-latitude westerly circulation on EASM circulation over both interannual [12] and millennial to orbital timescales [13].

Mid-latitude westerlies are dominated by 100- and 41-ka cycles and exhibit a dramatic transition from low amplitudes to high amplitudes at ~340 ka (Fig. 2b). Weaker westerlies are associated with anomalous upward motion over East Asia during the interglacial periods, while stronger westerlies are associated with downward motion during glacial periods (Fig. 2c). These effects arise when weakening of westerlies allows movement of cold air masses from high-latitude areas into East Asia. This increases development of fronts and convergence over East Asia where

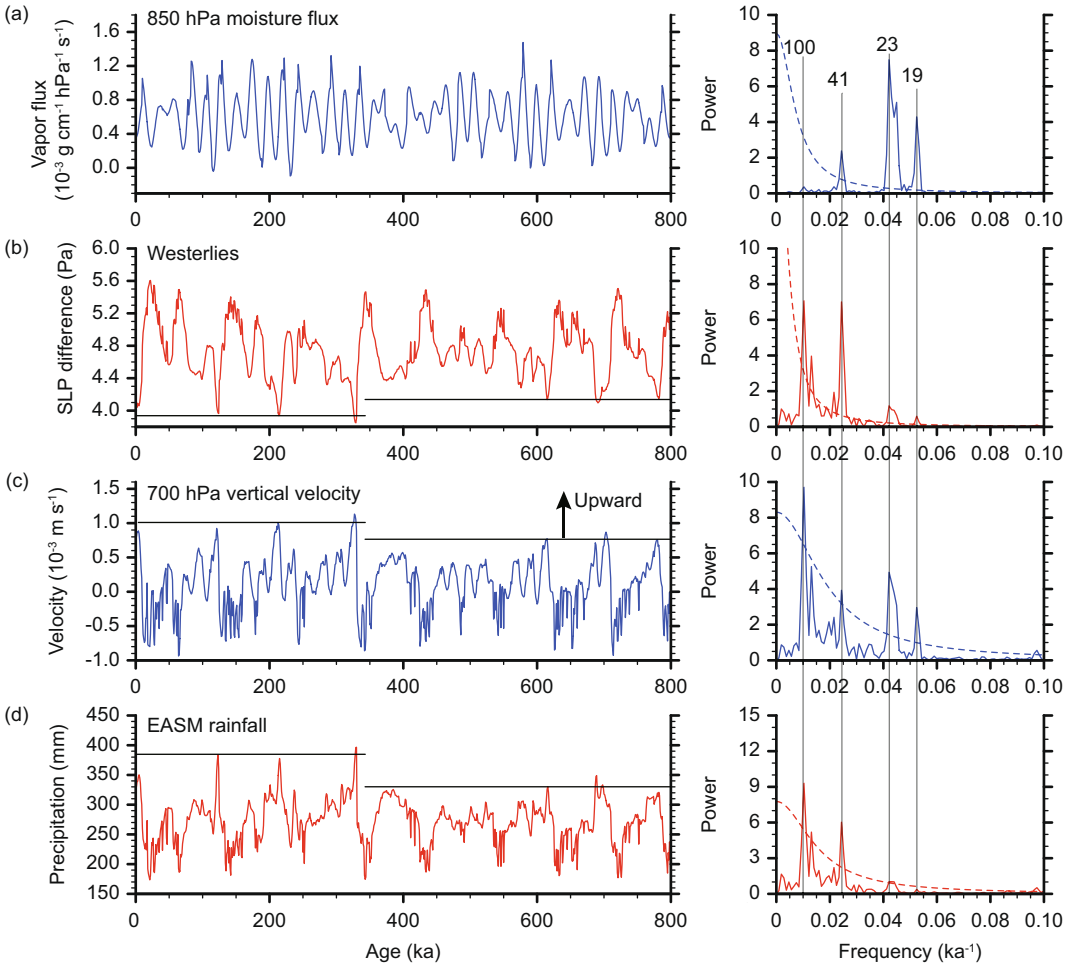

Fig. 2. (Color online) Forcing factors and EASM rainfall: time series (left panel) and spectra (right panel). (a) Simulated summer monsoonal moisture transport at 850 hPa over East Asia (10^{-3} g cm^{-1} hPa^{-1} s^{-1}). (b) Simulated summer westerly circulation (Pa) is defined as the normalized difference in global zonal-averaged sea level pressure (SLP) anomalies between 35° and 55°N. (c) Simulated summer vertical velocity at 700 hPa over East Asia (10^{-3} m s^{-1}). (d) Simulated EASM rainfall (mm). Dotted lines indicate the 95% confidence level (right panel). Black lines show the climatic transition in terms of the amplitude (left panel).

divergence typically prevails due to the WNPSH. Anomalous upward motion increases EASM rainfall during the interglacial periods, while downward motion decreases rainfall during glacial periods (Fig. 2d). Generally, glacial–interglacial changes in EASM rainfall likely reflect interactions between mid-latitude westerly circulation and WNPSH rather than EASM circulation alone.

EASM circulation and associated monsoonal moisture transport originate from thermal gradients between Asia and the North Pacific (Fig. S11a online). The land–sea thermal contrast develops directly from precession-induced local boreal summer insolation (Fig. S11b online) as high local insolation induces faster heating of land surfaces relative to sea surface. EASM circulation therefore tracks summer insolation and shows pronounced 23- and 19-ka cycles. Mid-latitude westerlies are triggered by thermal gradients between mid-latitude and subpolar regions (Fig. S11c online). These covary with atmospheric CO_2 concentrations (Fig. S4d, e online) and Northern Hemisphere ice sheets (Fig. S4b, c online). Compared with atmospheric CO_2 concentrations, ice sheets influence temperatures only to a minor and local degree at glacial–interglacial timescales [14]. Hence, variability in EASM rainfall with the 100- and 41-ka cycles depends strongly on changes in CO_2 concentration during the past 800 ka.

Loess and speleothem proxy records record different EASM patterns during the late Pleistocene-Holocene. The magnetic susceptibility of Chinese loess reflects the intensity of pedogenesis as governed by soil moisture and directly related to EASM rainfall [5]. Stalagmite $\delta^{18}O$ variation reflects the strength of monsoonal southerly winds transporting moisture towards East Asia from the tropical Pacific and Indian Oceans [4]. The simulation results described here give estimates for peak Holocene EASM intensity that might provide an explanation for the inconsistent of pollen and speleothem records. This suggests that loess (pollen) and speleothem records may represent fragmentary evidence of the EASM system as a whole.

Simulated EASM rainfall significantly differs from that simulated using the CCSM3 and the same CLIMBER-2 but with different protocols (Fig. S2 online). The present simulations considered interactions between Earth's climate system, while many simulations described in previous literatures neglect either climate feedback to forcing factors or interactions between the forcing factors. In the CLIMBER-2 simulations, Earth's orbital parameters are the only external factor. The observed 100-ka variation in EASM thus ultimately reflects orbital forcing and feedbacks of Earth's climate system including carbon cycle processes. Given the rather low resolution of the CLIMBER-2 model (Fig. S1 online), the simulation results described here do not resolve spatial differences in EASM rainfall that might influence model–proxy and model–model comparisons. The low resolution may also create regional artifacts in EASM results. While preliminary, the interpretations of the CLIMBER-2 simulation results given here demonstrate the potential of complex models and computational approaches in resolving Quaternary EASM dynamics and monsoon system science [15].

Conflict of interest

The authors declare that they have no conflict of interest.

Acknowledgments

This work was supported by the National Natural Science Foundation of China (42171152, 41775070, and 41920104005), the Fundamental Research Funds for the Central Universities (0209-14380107), and the Research Funds for the Frontiers Science Center for Critical Earth Material Cycling, Nanjing University. Four anonymous reviewers are sincerely thanked for their comments and constructive feedback which improved this paper.

Author contributions

Liya Jin and Xiaojian Zhang designed this study. Andrey Ganopolski and Matteo Willeit provided the simulation data and contributed to the discussion and paper revising. Huayu Lu and Fahu Chen contributed to the discussion of proxy records of loess, pollen and speleothem associated with the EASM (East Asian summer monsoon) evolution cycles. Xiaojian Zhang contributed to the data analysis and paper writing and prepared the figures. Liya Jin led the preparation of the manuscript and interpreted the results with contributions from all authors.

Appendix A. Supplementary materials

Supplementary materials to this short communication can be found online at https://doi.org/10.1016/j.scib.2023.04.004.

References

[1] Ding Y, Chan JCL. The East Asian summer monsoon: an overview. Meteorol Atmos Phys 2005;89:117–42.
[2] Cheng H, Zhang H, Cai Y, et al. Orbital-scale Asian summer monsoon variations: paradox and exploration. Sci China Earth Sci 2021;64:529–44.
[3] Sun Y, Wang T, Yin Q, et al. A review of orbital-scale monsoon variability and dynamics in East Asia during the Quaternary. Quat Sci Rev 2022;288:107593.
[4] Cheng H, Edwards RL, Sinha A, et al. The Asian monsoon over the past 640,000 years and ice age terminations. Nature 2016;534:640–6.
[5] Guo ZT, Berger A, Yin QZ, et al. Strong asymmetry of hemispheric climates during MIS-13 inferred from correlating China loess and Antarctica ice records. Clim Past 2009;5:21–31.
[6] Beck JW, Zhou W, Li C, et al. A 550,000-year record of East Asian monsoon rainfall from ^{10}Be in loess. Science 2018;360:877–81.
[7] Chen F, Xu Q, Chen J, et al. East Asian summer monsoon precipitation variability since the last deglaciation. Sci Rep 2015;5:11186.
[8] Cheng J, Wu H, Liu Z, et al. Vegetation feedback causes delayed ecosystem response to East Asian summer monsoon rainfall during the Holocene. Nat Commun 2021;12:1843.
[9] Willeit M, Ganopolski A, Calov R, et al. Mid-Pleistocene transition in glacial cycles explained by declining CO_2 and regolith removal. Sci Adv 2019;5:eaav7337.
[10] Lisiecki LE, Raymo ME. A Pliocene-Pleistocene stack of 57 globally distributed benthic $\delta^{18}O$ records. Paleoceanography 2005;20:PA1003.
[11] Lüthi D, Floch ML, Bereiter B, et al. High-resolution carbon dioxide concentration record 650,000–800,000 years before present. Nature 2008;453:379–82.
[12] Wu Z, Wang B, Li J, et al. An empirical seasonal prediction model of the East Asian summer monsoon using ENSO and NAO. J Geophys Res: Atmos 2009;114:D18120.
[13] Chiang JCH, Fung IY, Wu CH, et al. Role of seasonal transitions and westerly jets in East Asian paleoclimate. Quat Sci Rev 2015;108:111–29.
[14] Liu Z, Zhu J, Rosenthal Y, et al. The Holocene temperature conundrum. Proc Natl Acad Sci USA 2014;111:E3501–5.
[15] Cheng H, Li H, Sha L, et al. Milankovitch theory and monsoon. Innovation 2022;3:100338.

Liya Jin is a professor at School of Atmospheric Sciences, Chengdu University of Information Technology. His research interest focuses on Asian monsoon dynamics and paleoclimate simulation.

Xiaojian Zhang is an associate professor of Nanjing University. He received his Ph.D. degree from Lanzhou University in 2016. His research mainly focuses on paleoclimate modelling.